Journal of
Applied
Crystallography
ISSN 0021-8898

Received 16 August 2006
Accepted 11 April 2007

Structural formation and many-body effect of concentrated dendrimer solutions by computer simulations

Takamichi Terao

Department of Mathematical and Design Engineering, Gifu University, Japan. Correspondence e-mail: terao@gifu-u.ac.jp

Coarse-grained molecular dynamics simulations have been performed in order to study charged dendrimers in an aqueous solution. The structure factor, counterion distribution and effective interaction between molecules are clarified numerically. In particular, the many-body interactions in a triplet system are investigated, which is of importance in concentrated systems. These results shed new light on the analysis of recent small-angle X-ray and neutron scattering experiments on dendrimer solutions.

1. Introduction

Recently, the effective interaction and the phase behavior of *soft colloidal systems* have become subjects of strong interest. Star polymers, Gaussian particles and dendrimers are typical examples of soft colloids in an aqueous solution. Dendrimers are highly branched, tree-like macromolecules (Ballauf & Likos, 2004; Nisato *et al.*, 2000; Chen *et al.*, 2000). They are nano size with spherical shapes and are representative of soft colloidal particles. Dendrimers have numerous potential applications such as contrast agents for visualizing blood streams in magnetic resonance imaging and drug-delivery systems.

Several numerical studies have been devoted to the properties of many-body interactions to determine the structural formation in colloidal suspensions. Wu *et al.* have investigated three-body interactions among charged colloidal particles and their effect on phase behavior using Monte Carlo simulation (Wu *et al.*, 2000). They found that the three-body force can be repulsive or attractive, depending on macroion-to-macroion separation. Russ *et al.* have studied the pair and triplet interactions between charged colloidal spheres in an electrolyte solution within nonlinear Poisson–Boltzmann theory (Russ *et al.*, 2002). They have shown that pair interaction is repulsive, consistent with traditional Derjaguin–Landau–Verwey–Overbeek theory. However, the triplet potential is attractive, due to the presence of a charged colloidal particle between the other two particles that shields the direct repulsive interaction between the latter two. The phase behaviors of many-body interactions among dendrimer molecules are interesting topics, especially in a dense solution.

Soft matters are characterized by the coexistence of different characteristic length scales, such as microscopic and mesoscopic scales. It is very useful to employ coarse-grained approaches in computational soft-matter physics, and it is necessary to clarify the effective interaction between soft materials. This study performs coarse-grained molecular dynamics (MD) simulations to reveal the effective interaction and triplet force in dendrimer systems. It is demonstrated that triplet forces are repulsive in the case of charged dendrimers, in contrast to the case of hard-sphere, charged colloidal suspensions. The counterion distribution around dendrimers is clarified to determine how effectively they screen the electrostatic interaction in this system. It is indicated that most of the counterions exist within each dendrimer molecule.

2. Models

The conformation of dendrimers in an aqueous solution is studied using a stochastic MD method (Grest & Kremer, 1986). A coarse-grained model is introduced to describe dendrimer molecules and counterions are explicitly taken into account. The solvent is treated as a continuum which acts as a heat bath for the molecules and produces a viscous drag as each segment moves. The equation of motion for the ith segment with mass m is thus given by

$$m\frac{\mathrm{d}^2}{\mathrm{d}t^2}\mathbf{r}_i(t) = -\nabla U_i - m\Gamma\frac{\mathrm{d}}{\mathrm{d}t}\mathbf{r}_i(t) + \mathbf{W}_i(t), \qquad (1)$$

where Γ, $\mathbf{r}_i(t)$ and $\mathbf{W}_i(t)$ are the frictional coefficient that couples the monomers to the heat bath, the positional vector of the ith segment and the random force of the heat bath acting on each segment, respectively. $\mathbf{W}_i(t)$ is Gaussian white noise given by

$$\left\langle \mathbf{W}_i(t)\cdot\mathbf{W}_j(t')\right\rangle = 6mk_{\mathrm{B}}T\Gamma\delta_{ij}\delta(t-t'), \qquad (2)$$

where k_{B} and T are the Boltzmann constant and the temperature, respectively. The potential U_i consists of three terms

$$U_i = \sum_j U_{\mathrm{LJ}}(r_{ij}) + U_{\mathrm{FENE}} + U_{\mathrm{C}}, \qquad (3)$$

where r_{ij} is the distance between monomers i and j. In this equation, $U_{\mathrm{LJ}}(r)$ is the Lennard–Jones potential between any two particles, represented by

$$U_{\mathrm{LJ}}(r_{ij}) = \begin{cases} \varphi(r_{ij}) - \varphi(r_{\mathrm{c}}) & \text{for} \quad r_{ij} \le r_{\mathrm{c}} \\ 0 & \text{for} \quad r_{ij} > r_{\mathrm{c}} \end{cases}. \qquad (4)$$

Here, $\varphi(r_{ij})$ is defined to be

$$\varphi(r_{ij}) \equiv 4\varepsilon\Big[\big(\sigma/r_{ij}\big)^{12} - \big(\sigma/r_{ij}\big)^{6}\Big], \qquad (5)$$

where ε, σ and r_{c} are the unit of energy, particle diameter and cutoff radius, respectively. In addition, it is considered that counterions interact with each other and with monomers by the excluded-volume effect [$U_{\mathrm{LJ}}(r_{ij})$ in equation (3)] and by electrostatic interaction [U_{C} in equation (3)]. Charged monomers and counterions carry charges $+q$ and $-q$, respectively. To introduce the effect of solvent quality, the cutoff radius r_c is chosen to be $r_c = 2.5\sigma$ between monomer–monomer interactions and $r_c = 2^{1/6}\sigma$ otherwise. $U_{\rm FENE}$ denotes the bonding interaction between neighboring segments, given by

$$U_{\rm FENE}(r_{ij}) = \begin{cases} -0.5KR_0^2 \ln\left[1 - \left(r_{ij}/R_0\right)^2\right] & \text{for} \quad r_{ij} \le R_0 \\ 0 & \text{for} \quad r_{ij} > R_0 \end{cases}, \qquad (6)$$

where K is the bonding constant and R_0 is the maximum extension of the bond. In the following simulation, the values $R_0 = 1.5\sigma$ and $K = 30.0\varepsilon/\sigma^2$ are used where these parameters prevent bond crossings. Long-range Coulomb interaction $U_C(r_{ij})$ can be described by

$$\frac{U_C(r_{ij})}{k_B T} = \lambda_B \sum_{n_x=-\infty}^{\infty} \sum_{n_y=-\infty}^{\infty} \sum_{n_z=-\infty}^{\infty} \frac{z_i z_j}{\left|\mathbf{r}_{ij} + n_x L\mathbf{e}_x + n_y L\mathbf{e}_y + n_z L\mathbf{e}_z\right|}, \quad (7)$$

where $\mathbf{e}_x$, $\mathbf{e}_y$ and $\mathbf{e}_z$ are the unit vectors of the x, y and z directions, respectively. Here λ_B is the Bjerrum length which is given by $\lambda_B \equiv e^2/4\pi\varepsilon_d k_B T$ (ε_d is the dielectric constant of the medium). The temperature of the system is set to be $T = 300$ K. Periodic boundary conditions are imposed in the x, y and z directions, and the indices n_x, n_y and n_z, respectively, extend over the periodic images of the systems. The long-range nature of Coulomb interactions is numerically treated using the Lekner summation technique combined with particle-cell acceleration (Lekner, 1991).

Dendrimer molecules in a cubic box with periodic boundary conditions in all directions are considered. In the following, polyelectrolyte dendrimers such as polyamidoamine (PAMAM) dendrimers are considered (Lee *et al.*, 2002). The initial configuration of dendrimer molecules is built as follows. A segment of each chain is attached by self-avoiding random walks with a distance of $\sim\sigma$ in a cubic box having a system size of L. A dendrimer with M_G generations is built by adding $M_b - 1$ chains (of length M_l) to each of the free ends of a dendrimer with $M_G - 1$ generations, where M_b and M_l are the branching factor and the length per monomer between each branching point, respectively. The same procedure is continued in order to build dendrimers of the desired generation numbers.

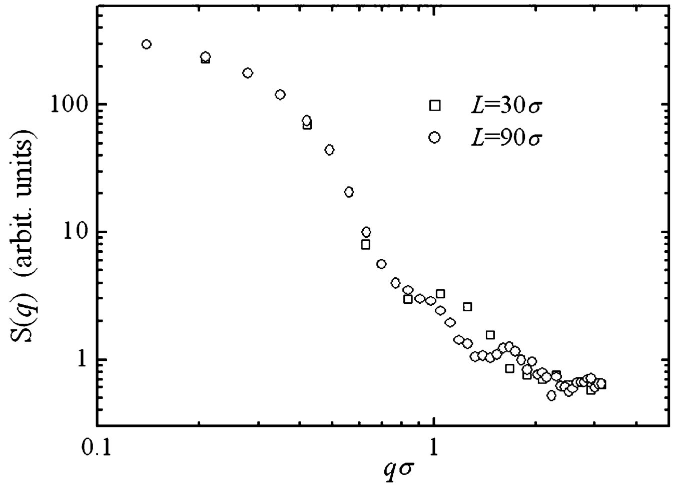

Figure 1
Structure factor $S(q)$ of charged dendrimers. The units of q are taken to be $1/\sigma$.

3. Numerical results

The generation of a dendrimer molecule M_G, a branching factor of M_b and the number of bonds between neighboring nodes of M_l are set to be $M_G = 4$, $M_b = 3$ and $M_l = 2$, respectively. The solvent effect is treated as a dielectric continuum with a relative dielectric constant of $\varepsilon_r = 78$. The temperature T, the frictional coefficient Γ and a time step δt are given to be $k_B T/\varepsilon = 1.2$, $\Gamma = 0.5\tau^{-1}$ and $\delta t = 0.002\tau$, respectively, where $\tau \equiv \sigma(m/\varepsilon)^{1/2}$ is the unit of time. In the following calculations, Monte Carlo (MC) simulation is employed with short MC steps ($\sim 10^5$ MCS) for structural relaxation, prior to MD simulations with large MD steps ($\ge 5 \times 10^5$ steps). First, we study the structural formation of *charged* dendrimer solutions, which have been recently investigated by small-angle X-ray scattering (SAXS) and small-angle neutron scattering experiments. The structure factor $S(\mathbf{q})$ is given by

$$S(\mathbf{q}) = \frac{1}{N}\left|\sum_{n=1}^{N} \exp(i\mathbf{q}\cdot\mathbf{r}_n)\right|^2, \qquad (8)$$

where N, $\mathbf{r}_n$ and $\mathbf{q}$ are the number of monomers, the position of nth monomer and the scattering vector, respectively. Here, the modulus of $\mathbf{q}$, q, is given by

$$q = \frac{4\pi}{\lambda}\sin\left(\frac{\theta}{2}\right), \qquad (9)$$

where θ and λ denote the scattering angle and the wavelength of the incident beam, respectively. In Fig. 1, the q dependence of the structure factor, $S(q)$, is shown for different system sizes. It is clarified that the calculated results with $L = 30\sigma$ and with $L = 90\sigma$ show good agreement with each other in the low-q regime, indicating that there is no serious finite-size effect. The ratios R_g/L for the system size $L = 30\sigma$ and $L = 90\sigma$ become 1.7×10^{-1} and 5.5×10^{-2}, respectively.

To observe how the counterions screen electrostatic repulsion between dendrimers, the counterion distribution around a dendrimer molecule is also studied. In general, the profile of counterions and their overlap greatly influence the effective interaction between dendrimers. The intermolecular density profile of dendritic polyelectrolytes has been studied to clarify whether the 'dense shell picture' or 'dense core picture' is valid on a charged dendrimer molecule. In Fig. 2, the profiles of monomer density $\rho(r)$, counterion density $\rho_c(r)$ and perimeter density $\rho_p(r)$ are shown with $M_G = 5$.

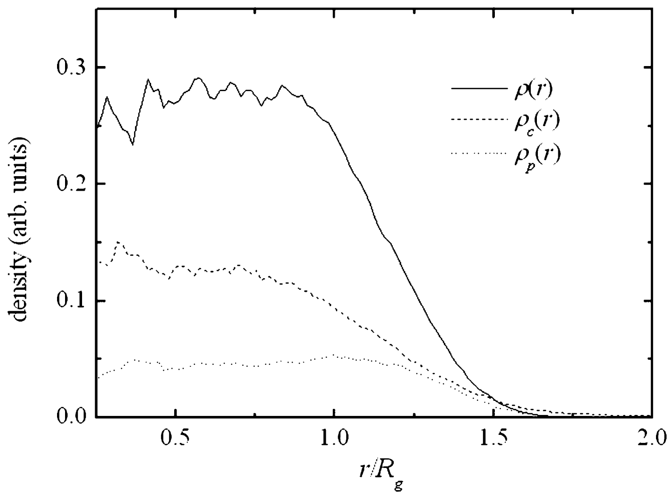

Figure 2
Profiles of monomer density $\rho(r)$, counterion density $\rho_c(r)$ and perimeter density $\rho_p(r)$.

Here r denotes the distance from the center of a dendrimer molecule, and $\rho_p(r)$ is the monomer density pertaining to the outermost monomers of the dendrimer molecule. It can be seen that the perimeter of a dendrimer is distributed not only at the surface of the spherical molecule but also inside the entire molecule, indicating that backfolding plays an important role in the conformation of charged dendrimers in an aqueous solution. We have to mention that this conclusion is limited to the case of a specific solvent quality in which the cutoff radius between monomer–monomer interactions r_c is given by $r_c = 2.5\sigma$. It is known that, in the absence of Coulombic interactions, this corresponds to a poor solvent condition. It is also shown that a portion of the counterions spread outside a dendrimer molecule. These results suggest that there is counterion overlap as well as monomer overlap when the distance between dendrimer molecules is smaller than $3R_g$.

The effective interaction between dendrimers provides useful information for understanding the phase behaviors in solution, which have been recently investigated using SAXS experiments (Ohshima *et al.*, 2001). A pair of dendrimer molecules is investigated which are confined in a cubic box of length L. The system size L is taken to be $L = 90\sigma$. The Debye screening length λ_D is estimated to be $\lambda_D \approx 2\sigma - 3\sigma$, thus the influence of the image-charged effect with periodic boundary conditions is negligibly small. A pair of dendrimers ($N = 2$) is placed symmetrically along the body diagonal of the cube, such that the center of the cube coincides with the center of mass of the two molecules. Their positions are denoted by $\mathbf{R}_1$ and $\mathbf{R}_2$ ($r \equiv |\mathbf{R}_1 - \mathbf{R}_2|$). Furthermore, the box contains N_c counterions carrying an opposite charge when the two dendrimer molecules are charged. Using MD simulations, the effective force $\mathbf{F}_i$ acting on each dendrimer molecule i ($i = 1, 2$) is calculated. Here $\mathbf{F}_i$ is defined as the force exerted onto the central monomer of each molecule. By symmetry, $\mathbf{F}_2 = -\mathbf{F}_1$, $\mathbf{F}_i$ is projected onto the body diagonal, defining

$$F^{(2)}(r) \equiv \left\langle \frac{\mathbf{F}_1 - \mathbf{F}_2}{2} \cdot \frac{\mathbf{R}_1 - \mathbf{R}_2}{|\mathbf{R}_1 - \mathbf{R}_2|} \right\rangle, \qquad (10)$$

where $\langle \ldots \rangle$ denotes the ensemble average. In equation (10), the effective interaction is repulsive when $F^{(2)}(r) > 0$ and *vice versa*. In addition, the three-body case of ($N = 3$) in a cubic box is also considered. The positions of the centers of the dendrimers are given such that they form an equilateral triangle of side length r. In this case, the positions $\mathbf{R}'_i$ and ($i = 1, 2, 3$) of the dendrimers are given by $\mathbf{R}'_1 \equiv (0, 0, 0)$, $\mathbf{R}'_2 \equiv (r, 0, 0)$ and $\mathbf{R}'_3 \equiv (r/2, \sqrt{3}r/2, 0)$, respectively. The projected force is defined by

$$F^{(3)}(r) \equiv \left\langle \frac{1}{3}\left(\frac{\mathbf{F}'_1(r) \cdot \mathbf{d}_1}{|\mathbf{d}_1|} + \frac{\mathbf{F}'_2(r) \cdot \mathbf{d}_2}{|\mathbf{d}_2|} + \frac{\mathbf{F}'_3(r) \cdot \mathbf{d}_3}{|\mathbf{d}_3|} \right) \right\rangle, \qquad (11)$$

where $\mathbf{d}_1 = (\sqrt{3}/2, 1/2, 0)$, $\mathbf{d}_2 = (-\sqrt{3}/2, 1/2, 0)$ and $\mathbf{d}_3 = (0, -1, 0)$, respectively. The magnitude of forces $F^{(2)}(r)$ and $F^{(3)}(r)$ are calculated by averaging over sufficiently long time steps.

Using MD simulations with $M_G = 5$ and $M_l = 2$ dendrimer molecules, the effective forces between dendrimers can be studied using equations (10) and (11). In Fig. 3, open squares and open circles show the calculated result of effective forces $F^{(2)}(r)$ with $N = 2$ and $F^{(3)}(r)$ with $N = 3$, respectively. The number of counterions N_c is taken to be $N_c = 508$ within a two-body system and $N_c = 762$ within a three-body system. The inset of Fig. 3 shows the triplet force $\Delta F(r)$ defined to be

$$\Delta F(r) \equiv F^{(3)}(r) - \sqrt{3}F^{(2)}(r), \qquad (12)$$

where $\sqrt{3}F^{(2)}(r)$ indicates the three-body force while neglecting the many-body effect. Fig. 3 shows that both the two-body force $F^{(2)}(r)$ and the three-body force $F^{(3)}(r)$ decay slowly as a function of distance r. In addition, the inset shows that the triplet force $\Delta F(r)$ becomes repulsive among charged dendrimer molecules. It is shown that the characteristics of the triplet force in this system are repulsive, indicating the importance of the nonlinear feature due to the excluded volume effect incorporated with the screened Coulomb effect on charged dendrimer monomers. Fig. 3 also shows that the ratio between $\Delta F(r)$ and $F^{(2)}(r)$ is approximately equal to $\Delta F(r)/F^{(2)}(r) \approx 0.3$ for $r < 2R_g$. These results indicate that both the overlap of monomers and that of counterions play an important role in determining the effective interaction, which is a specific feature of charged soft colloidal systems in an aqueous solution. This result is reminiscent of those of previous studies, indicating that the ratio $\Delta F(r)/F^{(2)}(r)$ becomes a constant value such as $\Delta F(r)/F^{(2)}(r) \approx -0.1$ on neutral star polymers (von Ferber *et al.*, 2000).

It is of great interest to explain why the triplet forces among charged dendrimers are so large and our interpretation is as follows: in charged dendrimer systems, each molecule consists of charged monomers and oppositely charged counterions, and almost all counterions accumulate inside the molecule. By counterion deformations among charged dendrimers, an electric dipole may be induced at each vertex of the equilateral triangle of side length r. It must be noted that that three induced electric dipoles cannot align in the same direction and a 'dipole–dipole interaction' becomes repulsive. It is assumed that not only the nonlinear screening effect, which has been discussed in previous studies, but also dipole–dipole interactions play an important role in determining the many-body interactions in these systems.

Recent studies have indicated that the triplet force among charged, hard-sphere colloids becomes attractive due to the nonlinear electrostatic screening effect (Dobnikar *et al.*, 2004; Hynninen *et al.*, 2004). It must be emphasized that the results of the present study do not contradict those of the previous numerical studies of charged, hard-sphere suspensions; if the separation distance between charged dendrimers is much larger than the gyration radius, soft colloidal particles can be approximately treated as a point-like charge. In this case, the image of charged, hard-sphere suspensions proposed by previous studies is recovered and the triplet force between charged dendrimers may become attractive due to the nonlinear screening effect in an aqueous solution. It is controversial whether the constant

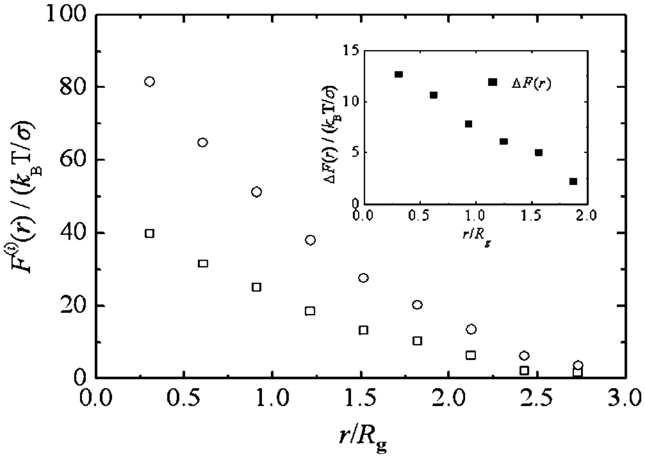

Figure 3

Effective forces $F^{(i)}(r)$ ($i = 2, 3$) in charged dendrimers; inset shows the profile of the triplet force $\Delta F(r) \equiv F^{(3)}(r) - \sqrt{3}F^{(2)}(r)$. Open squares and open circles show the calculated result of effective forces $F^{(2)}(r)$ with $N = 2$ and $F^{(3)}(r)$ with $N = 3$, respectively.

dielectric continuum approximation of the solvent is justified in this study. It must be mentioned that such an approach has a possible limitation in that the inter-monomer distances within a dendrimer are small and a linear-response theory may not be entirely applicable. Water molecules should be treated explicitly to clarify this issue and remain as a future problem.

4. Conclusions

To summarize, the properties of many-body interactions among charged dendrimers have been studied using stochastic MD simulations. It was clarified that the triplet force among charged dendrimers becomes repulsive, in contrast to that in charged, hard-sphere systems. These studies shed light on the characteristic features of soft colloidal systems, indicating that the structural formation of the self-assembly of charged dendrimers in a dense solution may differ considerably from those of hard-sphere suspensions. Hynninen *et al.* have performed a numerical study of the effect of attractive interaction on the phase behavior of suspensions of charged colloidal particles (Hynninen *et al.*, 2004). On the basis of free energy calculations, they have determined the phase diagram. It is indicated that the *bcc* phase is stabilized by long-range repulsions, and the inclusion of triplet attraction reduces the stability of the *bcc* phase. They concluded that the triplet interaction provides a significant effect on the phase diagram of charged colloidal suspensions. It is of great interest to clarify the phase diagram of 'soft colloidal crystals', which are produced from dense dendrimer solutions. The added-salt effect on the effective interaction between dendrimers should be investigated over a wide range of parameters; such studies are now in progress. In addition, direct experimental investigation concerning many-body interactions in dendrimer solutions is strongly desired, especially in concentrated systems. These investigations will also motivate the development of novel potential applications such as the encapsulation of guest molecules and the self-assembly of soft colloids such as nanocolloidal crystals. Future work will focus on controlling the self-assembly of dense nanoparticles, using soft colloidal particles having a large internal degree of freedom.

The authors thank the Supercomputer Center, Institute of Solid State Physics at the University of Tokyo for the use of their facilities. This work was supported in part by a grant-in-aid for scientific research from the Japan Ministry of Education, Culture, Sports, Science and Technology.

References

Ballauf, M. & Likos, C. N. (2004). *Angew. Chem. Int. Ed. Engl.* **43**, 2998–3020.

Chen, W., Tomalia, E. A. & Amis, E. J. (2000). *Macromolecules*, **33**, 9169–9172.

Dobnikar, J., Brunner, M., von Grünberg, H.-H. & Bechinger, C. (2004). *Phys. Rev. E*, **69**, 031402.

Ferber, C. von, Jusufi, A., Likos, C. N., Löwen, H. & Watzlawek, M. (2000). *Eur. Phys. J. E*, **2**, 311–318.

Grest, G. S. & Kremer, K. (1986). *Phys. Rev. A*, **33**, 3628–3631.

Hynninen, A.-P., Dijkstra, M. & van Roji, R. (2004). *Phys. Rev. E*, **69**, 061407.

Lee, I., Athey, B. D., Wetzel, A. W., Meixner, W. & Baker, J. R. Jr (2002). *Macromolecules*, **35**, 4510–4520.

Lekner, J. (1991). *Physica A*, **176**, 485–498.

Nisato, G., Ivkov, R. & Amis, E. J. (2000). *Macromolecules*, **33**, 4172–4176.

Ohshima, A., Konishi, T., Yamanaka, J. & Ise, N. (2001). *Phys. Rev. E*, **64**, 051808.

Russ, C., Grünberg, H. H., Dijkstra, M. & van Roij, R. (2002). *Phys. Rev. E*, **66**, 011402.

Wu, J. Z., Bratko, D., Blanch, H. W. & Prausnitz, J. M. (2000). *J. Chem. Phys.* **113**, 3360–3365.